Since January 2020 Elsevier has created a COVID-19 resource centre with free information in English and Mandarin on the novel coronavirus COVID-19. The COVID-19 resource centre is hosted on Elsevier Connect, the company's public news and information website.

Journal of Electronic Science and Technology 20 (2022) 100161

Contents lists available at ScienceDirect

Journal of Electronic Science and Technology

journal homepage: www.keaipublishing.com/en/journals/journal-of-electronic-science-and-technology/

Framework for COVID-19 segmentation and classification based on deep learning of computed tomography lung images

Wessam M. Salama [a], Moustafa H. Aly [b,*]

[a] Department of Basic Science, Faculty of Engineering, Pharos University, Alexandria, 12455, Egypt
[b] Department of Electronics and Communications Engineering, College of Engineering and Technology, Arab Academy for Science, Technology and Maritime Transport, Alexandria, 1029, Egypt

ARTICLE INFO

Keywords:
Augmentation
Classification
Computed tomography (CT)
Corona virus disease 2019 (COVID-19)
Deep learning
ResNet50
Segmentation
U-net
VGG16

ABSTRACT

Corona Virus Disease 2019 (COVID-19) has affected millions of people worldwide and caused more than 6.3 million deaths (World Health Organization, June 2022). Increased attempts have been made to develop deep learning methods to diagnose COVID-19 based on computed tomography (CT) lung images. It is a challenge to reproduce and obtain the CT lung data, because it is not publicly available. This paper introduces a new generalized framework to segment and classify CT images and determine whether a patient is tested positive or negative for COVID-19 based on lung CT images. In this work, many different strategies are explored for the classification task. ResNet50 and VGG16 models are applied to classify CT lung images into COVID-19 positive or negative. Also, VGG16 and ReNet50 combined with U-Net, which is one of the most used architectures in deep learning for image segmentation, are employed to segment CT lung images before the classifying process to increase system performance. Moreover, the image size dependent normalization technique (ISDNT) and Wiener filter are utilized as the preprocessing techniques to enhance images and noise suppression. Additionally, transfer learning and data augmentation techniques are performed to solve the problem of COVID-19 CT lung images deficiency, therefore the over-fitting of deep models can be avoided. The proposed frameworks which compromise of, end-to-end, VGG16, ResNet50, and U-Net with VGG16 or ResNet50, are applied on the dataset which is sourced from COVID-19 lung CT images in Kaggle. The classification results show that using the preprocessed CT lung images as the input for U-Net hybrid with ResNet50 achieve the best performance. The proposed classification model achieves 98.98% accuracy (ACC), 98.87% area under the ROC curve (AUC), 98.89% sensitivity (Se), 97.99% precision (Pr), 97.88% F_1-score, and 1.8974-second computational time.

1. Introduction

Corona Virus Disease 2019 (COVID-19) is an infectious disease that has affected more than millions of people worldwide and resulted in more than 6.3 million deaths (World Health Organization, June 2022) [1]. To alleviate the inefficiency and scarcity of current COVID-19 samples, a great deal of works have been placed into looking for alternate research methods. Several studies have shown that computed tomography (CT) scans reveal consistent radiological observations in COVID-19 patients [2]. Wide availability of CT devices makes testing more efficient and accessible. While CT imaging is useful for the diagnosis of COVID-19, reading the scans

* Corresponding author.
E-mail addresses: wessam.salama@pua.edu.eg (W.M. Salama), mosaly@aast.edu (M.H. Aly).

https://doi.org/10.1016/j.jnlest.2022.100161
Received 5 January 2021; Received in revised form 24 June 2022; Accepted 25 June 2022
Available online 30 June 2022

manually is time-consuming and subject to human errors. Therefore, advanced artificial intelligence (AI)-based automated image analysis is demanded to analyze CT scans in the assessment of COVID-19. AI-based image analysis methods can provide accurate and rapid diagnosis of the disease to cope with the demand for a large number of patients. For example, a manual assessment of a CT scan can take up to 15 min, while AI-based image analysis requires only a few seconds. Further, to alleviate the burden of medical professionals in reading CT scans, several works have developed deep learning methods that can automatically interpret CT images and predict whether the CT scans show positive for COVID-19 [3]. Although these studies show positive results, there are two drawbacks to them. First, because of privacy issues, the CT scan datasets used in such works are not sharable to the public. Therefore, their findings cannot be replicated and the models learned cannot be seen in other hospitals. Furthermore, the lack of an open-sourced annotated COVID-19 CT data collection significantly impedes training the deep learning models. Due to the low quality of COVID-19 CT lung images, some preprocessing techniques are applied to increase the quality of images.

A lot of research works for preprocessing techniques have been carried out in last two decades. The Gabor algorithmic filter technique was applied by Guo et al. [4]. The image size dependent normalization technique (ISDNT) [5] was used as a major part for enhancing the images. Previous studies [6,7] compared the efficiency of six image denoising techniques: the Gaussian filter, average filter, weighted average filter, Wiener filter, and median filter, showing that the Weiner filter provides the best results.

Impressive results have been achieved by using the deep learning algorithm [8] in the biomedical field, especially the deep convolutional neural networks (CNNs). For learning millions of parameters, deep CNNs require a large number of training images as well as the availability of its ground truth, which prevents many superior deep CNNs to be used in medical applications [9]. The U-Net model is the main architecture in segmentation, while both VGG16 and ResNet50 models are considered as powerful tools in image classification.

Data augmentation [10] is one of the applied techniques to overcome the scarcity of medical images. It expands the training data as new samples by applying a series of random transformations to existing data. It has the advantages of speeding up the convergence process, preventing over-fitting, and increasing generalization capabilities. Moreover, transfer learning [11] is defined as using a pre-trained model from one problem to solve another problem. This is more explained in subsection 3.5.

In [12], some algorithms were developed to describe deep learning, such as AlexNet, GoogLeNet [13], ResNet [14], VGG16, VGG19, and a U-Net model, for the classification and segmentation processes [15,16]. Since the COVID-19 epidemic, intensified attempts have been made to develop deep learning approaches to conduct the COVID-19 screening based diagnosis, such as using CT scans and chest X-rays to classify positive or negative COVID-19. Wu et al. set up an early-screening process focused on several CNN models to distinguish COVID-19 patients' CT scans [17]. Furthermore, CNN was used by Chowdhury et al. to classify COVID-19 patients based on X-ray images of the chest [18]. Several researches have used 3-dimensional (3D) deep learning models to view COVID-19 based on CT images from the chest [19] [-] [22]. The transfer-learning technique was utilized by Xu et al. [23] to develop the deep learning models. Shi et al. used the neural network "Visual Basic-Net (VB-Net)" for the CT scans to segment the COVID-19 infection regions [24]. Yu et al. have developed a U-Net++ based framework to classify COVID-19 patients using CT images [25]. Shen et al. introduced a random forest (iSARF) infection-size-aware approach that can automatically categorize subjects into classes of specific sets of infected lesion sizes [26]. However, latest methods in the literature have many cons and pros. One of the main cons is the need of large datasets and a lot of computational resources (memory and storage) for building and training CNNs. In our work, the dataset is limited, so it is not sufficient for building and training CNNs, but the data augmentation technique and transfer learning are applied to overcome the lack of tagged data and minimize the computational costs accordingly, increasing our frame work performance. However, CNNs still play an important role in medical filed diagnosis.

In this paper, VGG16 and ResNet50 models are used to distinguish positive and negative COVID-19 CT lung images results, while U-Net is used with both models to apply image segmentation for increasing the system efficiency. In addition to enhancements and noise suppression, preprocessing techniques, such as ISDNT and the Wiener filter are applied. Furthermore, system performance is improved by using transfer learning and data augmentation.

2. Methodology

The proposed framework is divided into four phases: 1) the preprocessing phase; 2) data augmentation and transfer learning; 3) segmentation based on the U-Net architecture; 4) classification based on VGG16 and ReseNet50 models. This work proposes techniques to segment and classify COVID-19 CT images into positive or negative. This work depends on utilizing the full power of pre-

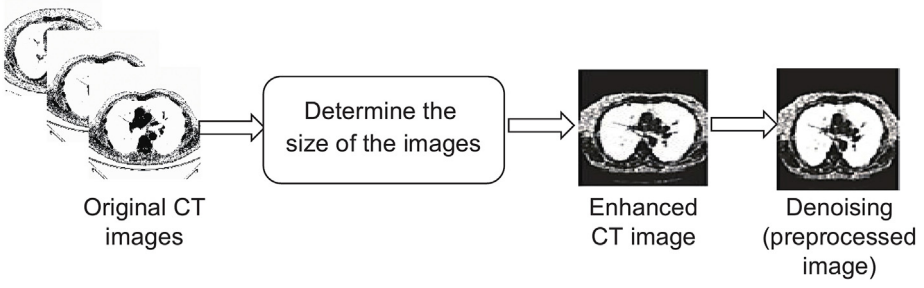

Fig. 1. Image preprocessing stage.

trained ResNet50 and VGG-16, as starting the training from scratch will lead to the over-fitting, time-consuming, and high-computational.

2.1. Image preprocessing phase

In the proposed algorithm, enhancing the image contrast and denoising are applied as the preprocessing step for the CT lung images. This step is performed to improve the image quality and therefore increase the images identification. In this paper, ISDNT [5] gives the best results. In addition, the Wiener filter [27] is utilized to denoise the CT lung images as explained in Fig. 1.

2.2. Data augmentation phase

We have already tried many strategies for data augmentation, including rotation and shifting [10]. Firstly, cropping, padding, and horizontal flipping are performed in our work. However, it is observed that after performing these data augmentation techniques, a part of the important information inside the CT images is lost, which affects the performance of the system. Secondly, another data augmentation technique is performed, in which our CT images are rotated 45°, 45° vertical flipped, and horizontal flipped. However, this data augmentation technique achieves less performance. Finally, some other rotation ways are performed in our work. Each pre-processed image rotates 0, 90°, 180°, and 270°, respectively. Therefore, each preprocessed image is augmented to four images as shown in Fig. 2. So, it is observed that the third raw in Fig. 2 is the optimal one. The results of the first and second two data augmentation techniques are added in Figs. 3 and 4.

2.3. Transfer learning

In this study, pre-trained VGG-16 and ResNet50 models [14,15] are used to produce higher performance than using these models starting from scratch. Training from scratch needs a huge number of datasets. So, using pre-trained models saves time and speeds up our suggested approach. Transfer learning is the process of using pre-trained models and modifying their parameters. This tackles the problem of small COVID-19 CT lung databases, which is our goal.

2.4. Segmentation phase

The segmentation of the region of interest (ROI) is a crucial step in the automated analysis of CT images for early detection. The segmentation could be considered as a classification task to classify each pixel in the dataset images either ROI or background (BG) [28].

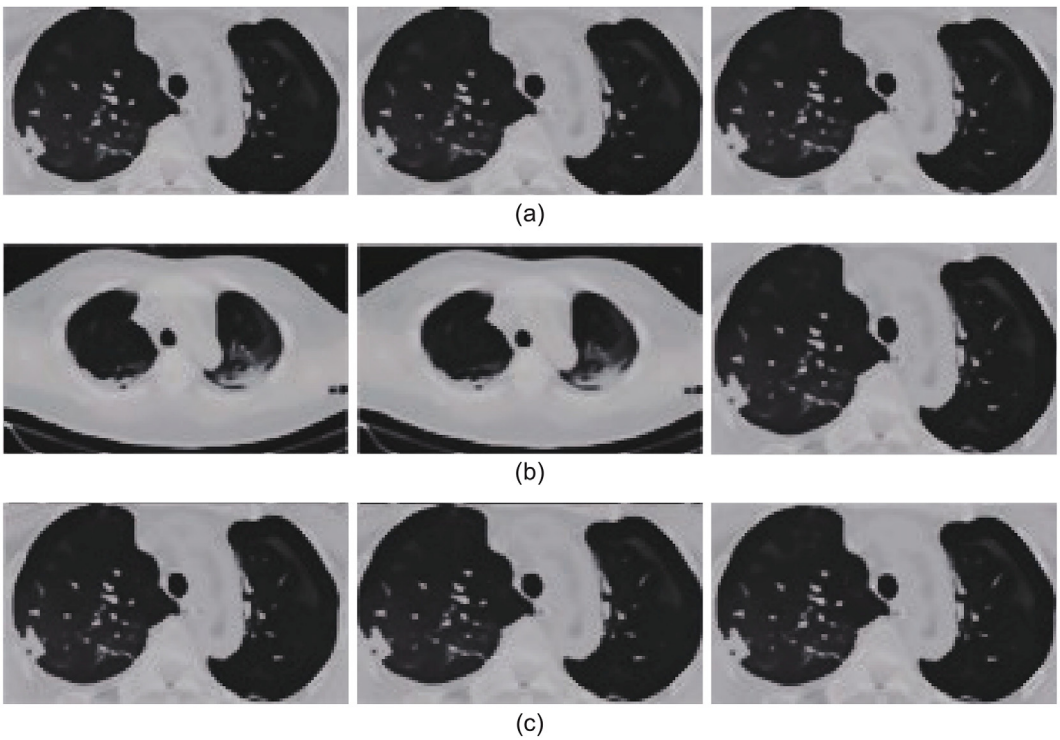

Fig. 2. Data augmentation: CT lung image rotation: (a) 90° rotation, (b) 180° rotation, and (c) 270° rotation.

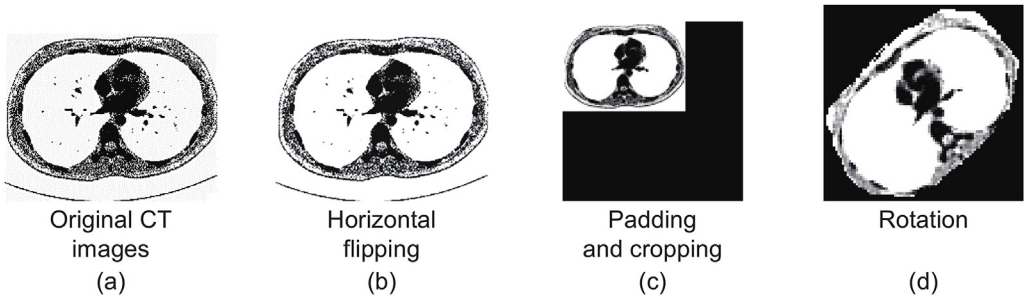

Fig. 3. Data augmentation: (a) original CT lung images, (b) horizontal flipping, (c) padding and cropping, and (d) rotation.

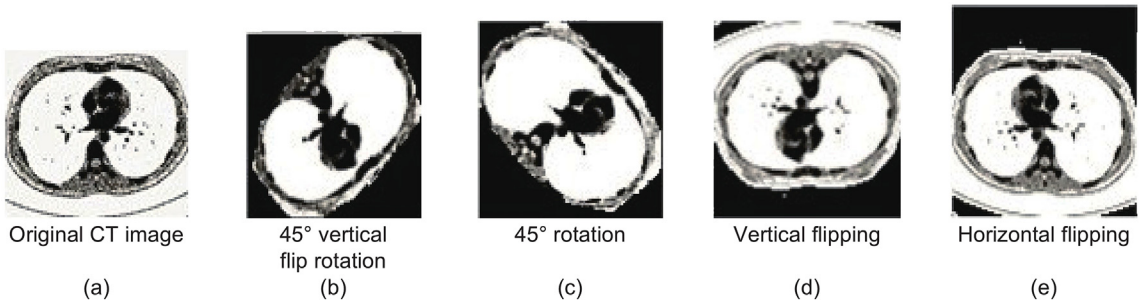

Fig. 4. Data augmentation: (a) original CT lung images, (b) 45° vertical flip rotation, (c) 45° rotation, (d) vertical flipping, and (e) horizontal flipping.

The input of this phase is the preprocessed COVID-19 CT lung images and the output is ROI segmented COVID-19 CT images. Then, the ROI images are masked with the original grayscale CT lung images as the input to the classifier phase. Fig. 5 explains the U-Net model. It consists of two paths with the same padding followed by the rectified linear unit (ReLU) and a 2 × 2-pixel max pool with the step of 2

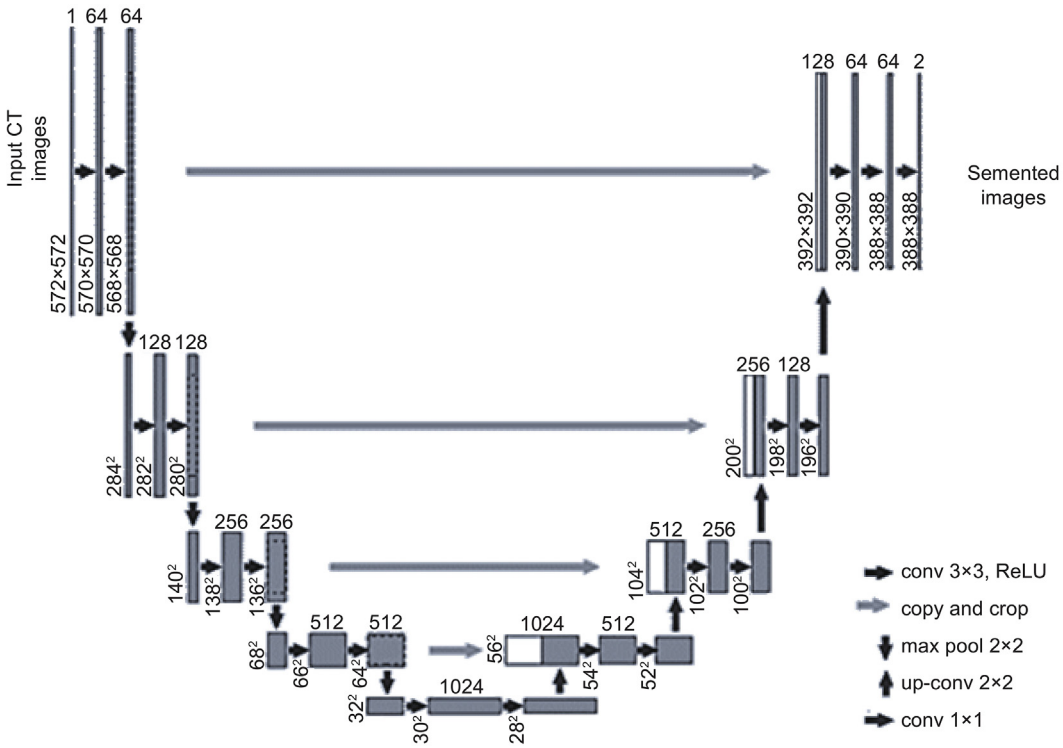

Fig. 5. U-Net architecture [15].

pixels [16], which are the basic elements of the U-Net based on the fully convolutional neural network (FCN) architecture, as the mixture of the layers of convolution in the contract direction and the layers of deconvolution in the expansive path. Segmented images of COVID-19 negative and positive images are showed in Figs. 6 and 7.

2.5. Classification phase based on deep CNN

Based on the obtained results in our previous work [14], it is observed that the ResNet50 and VGG16 models achieved the best performance in the classification process. The greyscale CT lung images are resized as 572 × 572 pixels, as explained in Fig. 5, to be suitable as the input of the proposed models. Our aim is to divide the COVID-19 CT images into two categories: Positive and negative. Some settings are tweaked to improve the performance of the COVID-19 CT image classification procedure. To begin, the parameters (the iteration number is 1×10^7, primary learning is adjusted to be 1×10^{-6}, the number of epoch is 150, the momentum is 0.9, and the weight decay is 5×10^{-4}) are fine-tuned to improve the performance, whereas prior parameters reflect the number of iterations, learning rate, number of epochs, momentum, and weight decay in the ResNet50 model. Second, to obtain the optimum performance, the iteration number, primary learning, epoch number, momentum, and weight decay should be 1×10^6, 1×10^{-5}, 200, 0.7, and 4×10^{-3}, respectively, in the VGG16 model. Tables 1 and 2 give more detailed descriptions of the deep convolution neural network algorithm.

3. Results

CT lung scans are promising in providing accurate, fast, and cheap screening and testing of COVID-19 [29]. Our collected COVID19-CT dataset consists of 349 COVID-19 CT and 397 non-COVID-19 CT. The dataset under investigation is split into two groups as follow: 70% for training and 30% for validation and testing based on patient IDs. These CT images have different sizes. The average, maximum and minimum heights are 491 pixels, 1853 pixels, and 153 pixels, respectively. The average, maximum, and minimum widths are 383 pixels, 1485 pixels, and 124 pixels, respectively. Our CT images are resized as 244 × 224 pixels to be suitable for our proposed deep learning models. Our research is based on Keras, a high-level Python library that runs smoothly on Notebook GPU cloud (2 CPU cores and 13 GB RAM).

Our proposed framework is implemented on 2312 total positive and negative COVID-19 CT lung images. All images under investigation are 2088 augmented CT images for training and 224 CT images for testing and validation, respectively. In order to authenticate the diagnosis results, different strategies are introduced, as shown in Tables 3 and 4. It is observed that the proposed framework using positive and negative COVID-19 CT lung databases with and without data augmentation achieves the best performance in terms of all metrics (the accuracy (ACC), sensitivity (Se), precision (Pr), F_1-score, and area under the ROC curve (AUC)).

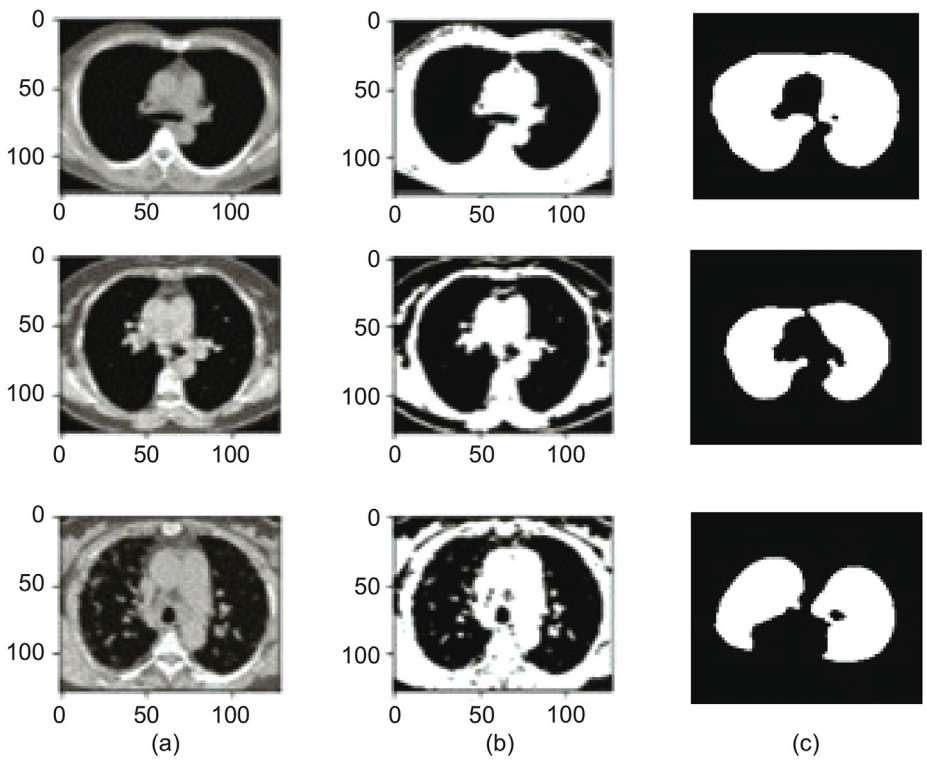

Fig. 6. Images segmentation of COVID-19 negative images: (a) original images, (b) segmented images, and (c) ground truth.

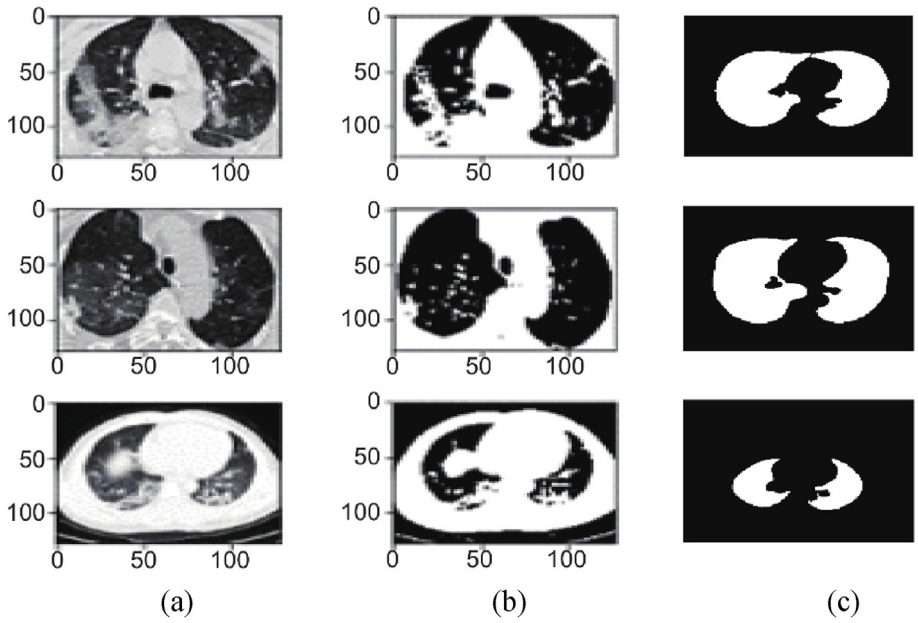

Fig. 7. Images segmentation of COVID-19 positive images: (a) original images, (b) segmented images, and (c) ground truth.

Table 1
Summary of the CNN layers for the ResNet50 architecture.

Layer No.	Type	Size	Kernel/Stride	Activation
/	Input	224 × 224 × 3	/	/
1	Convolution	64 × 3 × 3	2	ReLU
2	Convolution	1 × 1 × 64	2	ReLU
	Convolution	3 × 3 × 64		
	Convolution	1 × 1 × 256		
3	Convolution	1 × 1 × 128	2	ReLU
	Convolution	3 × 3 × 128		
	Convolution	1 × 1 × 512		
4	Convolution	1 × 1 × 256	2	ReLU
	Convolution	3 × 3 × 256		
	Convolution	1 × 1 × 1024		
5	Convolution	1 × 1 × 512	2	ReLU
	Convolution	3 × 3 × 512		
	Convolution	1 × 1 × 2048		
	Output	2	/	SVM

Table 2
Summary of the CNN layers for the VGG-16 architecture.

Layer No.	Type	Size	Kernel/Stride	Activation
/	Input	224 × 224 × 3	/	/
1	Convolution	64 × 3 × 3	2	ReLU
2	Convolution	1 × 1 × 64	2	ReLU
	Convolution	3 × 3 × 64		
	Convolution	1 × 1 × 256		
3	Convolution	1 × 1 × 128	2	ReLU
	Convolution	3 × 3 × 128		
	Convolution	1 × 1 × 512		
4	Convolution	1 × 1 × 256	2	ReLU
	Convolution	3 × 3 × 256		
	Convolution	1 × 1 × 1024		
5	Convolution	1 × 1 × 512	2	ReLU
	Convolution	3 × 3 × 512		
	Convolution	1 × 1 × 2048		
	Output	2	/	SVM

Table 3
Classification results for positive or negative COVID-19 without data augmentation for different phases (CT lung databases (LUNA16 and NLST) without data augmentation).

Model	ACC (%)	AUC (%)	Se (%)	Pr (%)	F_1-score (%)
VGG16	78.58	78.99	78.78	78.97	78.89
ResNet50	83.58	83.45	82.88	83.57	82.99
VGG16+ U-Net	86.78	87.85	86.98	87.43	86.59
ResNet50+ U-Net	89.48	89.45	88.98	88.57	88.99
Preprocessing + VGG16	85.48	85.45	84.98	85.57	84.99
Preprocessing + ResNet50	92.74	92.89	91.99	92.44	93.13
Preprocessing + U-Net + VGG16	94.89	94.99	94.88	95.43	95.12
Preprocessing + U-Net + ResNet50	96.88	96.87	95.99	95.78	96.46

Table 4
Classification results for positive or negative COVID-19 with data augmentation for different phases (CT lung databases (LUNA16 and NLST) with data augmentation).

Model	ACC (%)	AUC (%)	Se (%)	Pr (%)	F_1-score (%)
VGG16	80.68	80.89	80.78	80.97	80.92
ResNet50	85.88	85.45	85.95	85.82	85.99
VGG16+U-Net	88.58	87.85	87.98	88.43	88.59
ResNet50+ U-Net	90.68	90.45	89.99	90.57	89.99
Preprocessing + VGG16	87.98	88.95	87.98	88.77	87.99
Preprocessing + ResNet50	94.54	94.89	93.99	94.34	94.43
Preprocessing + U-Net + VGG16	96.79	95.99	96.78	96.53	96.82
Preprocessing + U-Net + ResNet50	98.98	98.87	98.89	97.99	97.88

To increase the total number of images, training images are augmented to four images using different directions of rotation to get a total number of 2312 CT images. The diagnosis performance is evaluated in terms of ACC, Se, Pr, F_1-score, AUC, and computational time. ACC is a measure of true predictions as in (1); Pr is the positive predictive value or fraction of detected malignant cases that match the ground truth, as in (2); Se is the true positive rate or the fraction of true malignant cases that are detected malignant, as in (3). F_1-score is the harmonic mean of Pr and Se and it represents a more generalized form balancing both, which gives the sample sets, similarity and diversity as represented in (4). And AUC can be obtained directly from the results (without a definition equation). It measures the entire two-dimensional area under the entire ROC curve and it provides an aggregate measure of performance across all possible classification thresholds. Except AUC, the mentioned metrics are defined as follows [30]:

$$\mathrm{ACC} = (\mathrm{TP} + \mathrm{TN}) / (\mathrm{TP} + \mathrm{FP} + \mathrm{TN} + \mathrm{FN}) \tag{1}$$

$$\mathrm{Pr} = \mathrm{TP} / (\mathrm{TP} + \mathrm{FP}) \tag{2}$$

$$\mathrm{Se} = \mathrm{TP} / (\mathrm{TP} + \mathrm{FN}) \tag{3}$$

$$F_1\text{-score} = 2(\mathrm{Pr} \times \mathrm{Se})/(\mathrm{Pr} + \mathrm{Se}) \tag{4}$$

where FP is the non-lesion pixel segmented as the lesion pixel, which denotes the false positive; FN is the lesion pixel segmented as the non-lesion pixel, which denotes the false negative. TP is the true positive and TN is the true negative.

Tables 3 and 4 show the COVID-19 classification results for the CT lung images by using the proposed classification models. To assess

Table 5
A comparison between several classification methods based on different CNN architectures, datasets, and our proposed models.

Model	Dataset	Total number of images	ACC (%)	F_1-score (%)	AUC (%)
Our proposed framework Preprocessing + U-Net + ResNet50	COVID-19 CT images	2312	98.98	97.88	98.87
Our proposed framework Preprocessing + ResNet50	COVID-19 CT images	2312	94.54	94.43	94.89
Our proposed framework ResNet50+ U-Net	COVID-19 CT images	2312	90.68	89.99	90.45
Our proposed framework ResNet50	COVID-19 CT images	2312	85.88	85.99	85.45
VGG-16 [30]	COVID-19 CT images	746	76.00	76.00	82.00
ResNet-50 [30]	COVID-19 CT images	746	83.00	85.00	91.00
DenseNet-169 [30]	COVID-19 CT images	746	86.00	85.00	94.00
DenseNet-169 [31]	COVID-CT-349 images	812	87.10	88.10	95.20
ResNet-50 [31]	COVID-CT-349 images	812	77.40	74.60	86.40

the impact for each of the four phases on the proposed classification framework, the performance is evaluated for the following models individually:

- VGG16 and ResNet50 classify the CT images into positive or negative COVID-19.
- U-Net for segmenting, then VGG16 and ResNet50 classify the segmented CT images into positive or negative COVID-19.
- After preprocessing for the CT images using ISDNT and the Wiener filter, then the classification is performed by the VGG16 and ResNet50.
- Preprocessing is followed by the U-Net segmentation network, and then the VGG16 and ResNet50 classification networks work.

Also, for proving the influence of the data augmentation technique on the models performance, the classifier performance with and without data augmentation is explored, as shown in Tables 3 and 4

The proposed framework for positive or negative COVID-19 CT lung classification is compared with other recent systems [31,32], and the results are shown in Table 5. The results show that the better performance is achieved by the proposed frameworks, as shown in Table 5.

4. Conclusions

In this paper, different strategies, end-to-end, VGG16 and ResNet50 are applied to classify lung CT images into positive or negative COVID-19. Then, the U-Net with VGG16 or ResNet50 models are performed to segment and classify lung CT images into positive or negative COVID-19. In addition, preprocessing techniques are used to improve the image quality and remove noise. And data augmentation and transfer learning are applied to overcome the lack of the tagged COVID-19 dataset.

The diagnosis performance is evaluated in terms of AUC, ACC, Se, Pr, F_1-score, and computational time. Experimental results show that the strategy using preprocessing, U-Net combined with the ResNet50 architecture, and data augmentation provides very accurate classification results with the average AUC of 98.87%, ACC of 98.98%, Se of 98.89%, Pr of 97.99%, and F_1-score of 97.88% for the used database, and the computation memory requirement of this strategy is as low as possible. The results highlight the positive impact of using data augmentation and transfer learning in enhancing the classification performance. The robustness of the proposed system is investigated by comparing it with other recent COVID-19 classification systems, and the results reveal the superior performance of the proposed approach.

Declaration of competing interest

The authors declare no conflict of interest.

Appendix A. Supplementary data

Supplementary data to this article can be found online at https://doi.org/10.1016/j.jnlest.2022.100161.

References

[1] WHO, Coronavirus Disease (COVID-19) dashboard [Online]. Available: https://covid19.who.int/?gclid=EAIaIQobChMI3tGszJC76QIVh_hRCh2jFg4nEAAYASAAEgLmr_D_BwE.2020.
[2] A. Bernheim, X.-Y. Mei, M.-Q. Huang, et al., Chest CT findings in coronavirus disease-19 (COVID-19): relationship to duration of infection, Radiology 295 (3) (Feb. 2020) 685–691.
[3] X.-W. Xu, X. Jiang, C.-L. Ma, et al., A deep learning system to screen novel Coronavirus Disease 2019 pneumonia, Engineering 6 (10) (2020) 1122–1129.
[4] Y.-M. Guo, Y. Liu, A. Oerlemans, S.-Y. Lao, S. Wu, M.S. Lew, Deep learning for visual understanding: a review, Neurocomputing 187 (Apr. 2016) 27–48.
[5] D.A. van Dyk, X.-L. Meng, The art of data augmentation, Journal of Computational and Graphical Statistics 10 (1) (Mar. 2001) 1–50.
[6] M.S. Al-Tarawneh, Lung cancer detection using image processing techniques, Leonardo Electronic Journal of Practices and Technologies 11 (20) (2012) 147–158.
[7] S.M. Sandeep, Enhancement on low contrast bird images using image size dependent normalization technique, Intl. Journal of Advanced Research in Computer Science 8 (8) (2017) 628–631.
[8] A. Shrestha, A. Mahmood, Review of deep learning algorithms and architectures, IEEE Access 7 (Apr. 2019) 53040–53065.
[9] M.T. McCann, K.H. Jin, M. Unser, Convolutional neural networks for inverse problems in imaging: a review, IEEE Signal Processing Magazine 34 (6) (Nov. 2017) 85–95.
[10] X. Li, W. Zhang, Q. Ding, J.-Q. Sun, Intelligent rotating machinery fault diagnosis based on deep learning using data augmentation, Journal of Intelligent Manufacturing 31 (2) (2020) 433–452.
[11] S.J. Pan, Q. Yang, A survey on transfer learning, IEEE Trans. on Knowledge and Data Engineering 22 (10) (2010) 1345–1359, Oct.
[12] G. Hinton, Deep learning-a technology with the potential to transform health care, JAMA 320 (11) (2018) 1101–1102, Sept.
[13] S.G. Lee, Y. Sung, Y.G. Kim, E.Y. Cha, Variations of AlexNet and GoogLeNet to improve Korean character recognition performance, Journal of Information Processing Systems 14 (1) (Feb. 2018) 205–217.
[14] W.M. Salama, A.M. Elbagoury, M.H. Aly, Novel breast cancer classification framework based on deep learning, IET Image Processing 14 (13) (2020) 3254–3259, Nov.
[15] X.-Y. Zhang, J.-H. Zou, K.-M. He, J. Sun, Accelerating very deep convolutional networks for classification and detection, IEEE Trans. on Pattern Analysis and Machine Intelligence 38 (10) (2016) 1943–1955, Oct.
[16] O. Ronneberger, P. Fischer, T. Brox, U-Net: convolutional networks for biomedical image segmentation, in: Proc. Of the 18th Intl. Conf. on Medical Image Computing and Computer-Assisted Intervention, 2015, pp. 234–241. Munich.

[17] Q.-Q. Ni, Z.-Y. Sun, L. Qi, et al., A deep learning approach to characterize 2019 Coronavirus Disease (COVID-19) pneumonia in chest CT images, European Radiology 30 (12) (2020) 6517–6527, Jul.
[18] C.-S. Zheng, X.-B. Deng, Q. Fu, et al., Deep learning-based detection for COVID-19 from chest CT using weak label [Online]. Available: https://www.medrxiv.org/content/10.1101/2020.03.12.20027185v2, March 2020.
[19] Y. Deng, L. Lei, Y. Chen, W. Zhang, The potential added value of FDG PET/CT for COVID-19 pneumonia, European Journal of Nuclear Medicine and Molecular Imaging 47 (7) (2020) 1634–1635, Mar.
[20] D. Singh, V. Kumar, M. Kaur, Classification of COVID-19 patients from chest CT images using multi-objective differential evolution-based convolutional neural networks, European Journal of Clinical Microbiology & Infectious Diseases 39 (7) (2020) 1379–1389, Apr.
[21] L. Li, L.-X. Qin, Z.-G. Xu, et al., Artificial Intelligence Distinguishes Covid-19 from Community Acquired Pneumonia on Chest CT, Radiology, Mar. 2020, p. 200905, 1-8.
[22] Y. Song, S.-J. Zheng, L. Li, et al., Deep learning enables accurate diagnosis of novel coronavirus (COVID-19) with CT images, IEEE/ACM Trans. on Computational Biology and Bioinformatics 18 (6) (2020) 2775–2780.
[23] S. Wang, B. Kang, J.-L. Ma, et al., A deep learning algorithm using CT images to screen for Corona Virus Disease (COVID-19), European Radiology 31 (8) (2020) 6096–6104, Aug.
[24] H.-T. Zhang, J.-S. Zhang, H.-H. Zhang, et al., Automated detection and quantification of COVID-19 pneumonia: CT imaging analysis by a deep learning-based software, European Journal of Nuclear Medicine and Molecular Imaging 47 (11) (2020) 2525–2532, Oct.
[25] J. Chen, L.-L. Wu, J. Zhang, et al., Deep learning-based model for detecting 2019 novel coronavirus pneumonia on high-resolution computed tomography: a prospective study [Online]. Available: https://www.medrxiv.org/content/10.1101/2020.02.25.20021568v1, February 2020.
[26] F. Shi, L.-M. Xia, F. Shan, et al., Large-scale screening of covid-19 from community acquired pneumonia using infection size-aware classification [Online]. Available: https://arxiv.org/abs/2003.09860, March 2020.
[27] J.S. Goldstein, I.S. Reed, L.L. Scharf, A multistage representation of the Wiener filter based on orthogonal projections, IEEE Trans. on Information Theory 44 (7) (1998) 2943–2959, Nov.
[28] M.B. Tayel, A.M. Elbagoury, Breast infrared thermography segmentation based on adaptive tuning of a fully convolutional network, Current Medical Imaging 16 (5) (May 2020) 611–621.
[29] A CT scan dataset about COVID-19 [Online]. Available: www.Kaggle.com, 2020.
[30] T. Saito, M. Rehmsmeier, Precrec: fast and accurate precision–recall and ROC curve calculations in R, Bioinformatics 33 (1) (Jan. 2017) 145–147.
[31] X.-H. He, X.-Y. Yang, S.-H. Zhang, et al., Sample-efficient deep learning for COVID-19 diagnosis based on CT scans [Online]. Available: https://www.medrxiv.org/content/10.1101/2020.04.13.20063941v1, April 2020.
[32] X.-Y. Yang, X.-H. He, J.-Y. Zhao, Y.-C. Zhang, S.-H. Zhang, P.-T. Xie, COVID-CT-dataset: a CT Scan dataset about COVID-19 [Online]. Available: https://arxiv.org/abs/2003.13865, June 2020.

Wessam M. Salama received the B.Sc. degree in Electrical Engineering, M.Sc. and Ph.D. degrees in Electrical Engineering from Alexandria University in Egypt in 2008, 2013 and 2018 respectively. She is currently a Teacher assistant at the Engineering Mathematics and Physics department, Pharos University. Her main research interests are in information security and computer applications in biomedical engineering. She has over four publications in these fields.

Moustafa H. Aly was born in 1953, Alexandria, Egypt. He received his B.Sc., M.Sc. and Ph.D. from Faculty of Engineering, Alexandria University, Alexandria, Egypt, respectively in 1976, 1983 and 1987. He is a professor of Optical Communications, Electronics and Communications Engineering Department, College of Engineering and Technology, Arab Academy for Science, Technology and Maritime Transport, Alexandria, Egypt. He was a co-supervisor of 140 M.Sc. and Ph.D. students and published 340 journal and conference papers. His research area includes Machine Learning, Optical Communications, Optical Amplifiers, Free Space Optics, Visible Light Communications, and Optical Networks, Communications.